

Video Article

# Fundus Photography as a Convenient Tool to Study Microvascular Responses to Cardiovascular Disease Risk Factors in Epidemiological Studies

Patrick De Boever<sup>1,2</sup>, Tijs Louwies<sup>1,2</sup>, Eline Provost<sup>1,2</sup>, Luc Int Panis<sup>1,3</sup>, Tim S. Nawrot<sup>2,4</sup>

<sup>1</sup>Environmental Risk and Health, Flemish Institute for Technological Research (VITO)

<sup>2</sup>Centre for Environmental Sciences, Hasselt University

<sup>3</sup>Transportation Research Institute, Hasselt University

<sup>4</sup>Department of Public Health, Occupational and Environmental Medicine, Leuven University

Correspondence to: Patrick De Boever at [patrick.deboever@vito.be](mailto:patrick.deboever@vito.be)

URL: <http://www.jove.com/video/51904>

DOI: [doi:10.3791/51904](https://doi.org/10.3791/51904)

**Keywords:** Medicine, Issue 92, retina, microvasculature, image analysis, Central Retinal Arteriolar Equivalent, Central Retinal Venular Equivalent, air pollution, particulate matter, black carbon

Date Published: 10/22/2014

**Citation:** De Boever, P., Louwies, T., Provost, E., Int Panis, L., Nawrot, T.S. Fundus Photography as a Convenient Tool to Study Microvascular Responses to Cardiovascular Disease Risk Factors in Epidemiological Studies. *J. Vis. Exp.* (92), e51904, doi:10.3791/51904 (2014).

## Abstract

The microcirculation consists of blood vessels with diameters less than 150  $\mu\text{m}$ . It makes up a large part of the circulatory system and plays an important role in maintaining cardiovascular health. The retina is a tissue that lines the interior of the eye and it is the only tissue that allows for a non-invasive analysis of the microvasculature. Nowadays, high-quality fundus images can be acquired using digital cameras. Retinal images can be collected in 5 min or less, even without dilatation of the pupils. This unobtrusive and fast procedure for visualizing the microcirculation is attractive to apply in epidemiological studies and to monitor cardiovascular health from early age up to old age.

Systemic diseases that affect the circulation can result in progressive morphological changes in the retinal vasculature. For example, changes in the vessel calibers of retinal arteries and veins have been associated with hypertension, atherosclerosis, and increased risk of stroke and myocardial infarction. The vessel widths are derived using image analysis software and the width of the six largest arteries and veins are summarized in the Central Retinal Arteriolar Equivalent (CRAE) and the Central Retinal Venular Equivalent (CRVE). The latter features have been shown useful to study the impact of modifiable lifestyle and environmental cardiovascular disease risk factors.

The procedures to acquire fundus images and the analysis steps to obtain CRAE and CRVE are described. Coefficients of variation of repeated measures of CRAE and CRVE are less than 2% and within-rater reliability is very high. Using a panel study, the rapid response of the retinal vessel calibers to short-term changes in particulate air pollution, a known risk factor for cardiovascular mortality and morbidity, is reported. In conclusion, retinal imaging is proposed as a convenient and instrumental tool for epidemiological studies to study microvascular responses to cardiovascular disease risk factors.

## Video Link

The video component of this article can be found at <http://www.jove.com/video/51904/>

## Introduction

The microcirculation consists of blood vessels with diameters less than 150  $\mu\text{m}$  and includes smallest resistance arteries, arterioles, capillaries, and venules. These vessels make up a large part of the circulatory system and play an important role in maintaining cardiovascular health. The vessel diameter of 150  $\mu\text{m}$  is a physiological and a physical limit. The rheological properties of vessels with a diameter less than 150  $\mu\text{m}$  differ from large arteries. Furthermore, most of the autoregulatory resistance changes occur downstream from 150  $\mu\text{m}$  in vascular beds exhibiting blood flow autoregulation<sup>1</sup>. The microcirculation has two important functions. The primary function is to provide cells with oxygen and metabolic substrates in order to match tissue demand and to drain waste products and carbon dioxide. Alterations in the number of exchange vessels and the microvascular flow patterns reduces the effective exchange surface area and may lead to suboptimal tissue perfusion and a failure to meet metabolic demand<sup>2</sup>. Further, the hydrostatic pressure drops within the vascular bed and the microcirculation plays a role in regulating the overall peripheral resistance<sup>3</sup>.

The retina is a layered tissue lining the interior of the eye. Its main function is to convert the incoming light into a neural signal that is further propagated to the visual cortex for processing visual information. The function of the retina is to see the outside world and all the ocular structures involved in this process are optically transparent. This makes the retinal tissue accessible for non-invasive imaging of the microvasculature<sup>4</sup>. Retinal imaging is being used to identify diseases of the eye. For example, an advanced form of macular degeneration can lead to vision loss because of abnormal blood vessel growth into the macula. These blood vessels tend to be more permeable and subject to bleeding and leaking of blood and proteins within or below the retina. The latter events are responsible for the irreversible damage to the photoreceptors. Development of glaucoma correlates with a damaging of ganglion cells and their axons. The effect of this process leads to cupping of the optic disc, which can be observed in retinal images<sup>5</sup>. Diabetic retinopathy is caused by hyperglycemia that leads to damage in the

retinal vessel walls. This can result in ischemia, the growth of new blood vessels and a change in the vascular geometric network. Furthermore, the blood-retinal barrier may be subject to breakdown, causing leakage of dilated hyperpermeable capillaries and aneurysms<sup>6</sup>.

Retinal microvasculature shows homology with the microvascular beds found in the heart, lungs, and brain<sup>7</sup>. It is established that systemic diseases that affect the microcirculation of the brain can cause parallel changes in the retina. Arteriolar narrowing and enhanced arteriolar light reflex of the retina is associated with vessel abnormalities, white matter lesions and lacunes that are caused by cerebral small vessel disease<sup>8</sup>. A significant relationship was discovered between narrower retinal venules, an altered retinal microvascular network and the occurrence of Alzheimer disease. It is suggested that brains of patients have an altered cerebral microvasculature that is also observable in the retina<sup>9</sup>.

Evidence is also increasing about the correlation between retinal vascular changes and coronary heart disease<sup>10,11</sup>. The ratio between the diameter of retinal arteries and retinal veins (A/V) has been shown to be a sensitive proxy to reflect hypertension and atherosclerosis<sup>12</sup>. A narrowing of the arteries and widening of the veins, leading to a decreased A/V ratio, corroborates risk of stroke and myocardial infarction<sup>13</sup>. Hypertension can cause direct retinal ischemia and retinal infarcts that become visible as cotton wool spots and deep retinal white spots<sup>14</sup>. Serre and Sasongko recently summarized the literature and they concluded that exposure to lifestyle and environmental risk factors (e.g., diet, physical activity, smoking, and air pollution) can induce morphological changes in the retinal microvascular bed<sup>15</sup>. Importantly, such retinal changes have been associated with cardiovascular risk factors, even before clinical manifestations of diseases<sup>16</sup>.

Significant increases in the incidence of cardiovascular morbidity and mortality have been attributed to long- and short-term exposures to particulate matter air pollution<sup>17,18</sup>. Research indicates that particulate matter (PM), an important fraction of air pollution, contributes to the development of cardiovascular disease and induces cardiovascular events<sup>19,20</sup>. An impairment of the function of the microvascular bed is thought to play a role in the observed associations. In this respect, an association between exposure to air pollution and arteriolar narrowing in the retina has been reported by Adar and colleagues<sup>21</sup>. The retinal arteriolar caliber was narrower and venular caliber was wider among the 4607 participants of the Multi-Ethnic Study of Atherosclerosis (MESA) that were living in areas with increased long- and short-term exposure to PM<sub>2.5</sub> (particulate matter  $\leq 2.5$   $\mu\text{m}$  in diameter)<sup>21</sup>. Systemic inflammation caused by chronic air pollution exposure may result in wider venular diameters<sup>22</sup>. This corroborates the studies that report the impact of smoking on the retinal microvascular bed<sup>23</sup>. A recent publication reports on the association between short-term air pollution exposure and microvascular changes in healthy adults (22-63 years of age) measured with retinal fundus photography<sup>24</sup>. An increase in PM<sub>10</sub> (particulate matter  $\leq 10$   $\mu\text{m}$  in diameter) and BC (black carbon, a combustion by-product that can be used as a proxy for traffic-related diesel exhaust) was associated with a decrease in arteriolar caliber<sup>24,25</sup>.

In this scientific video protocol, the procedures are described to collect fundus pictures of the eye, to perform image analysis to obtain arteriolar and venular vessel calibers, and to calculate Central Retinal Arteriolar Equivalent (CRAE) and Central Retinal Venular Equivalent (CRVE). Retinal imaging is gaining increased attention because the retina is the only tissue that allows an unobtrusive analysis of the microvasculature and images can be collected from early age up to old age<sup>26,27</sup>. CRAE and CRVE appear to be sensitive parameters that reflect the impact of modifiable lifestyle and environmental cardiovascular disease risk factors on the microvasculature. In the manuscript, the repeatability of the vessel analysis is demonstrated. Furthermore, the applicability of retinal microvasculature analysis in epidemiological studies is shown by summarizing our findings obtained in a repeated-measures design with a focus on the impact of particulate air pollution exposure<sup>24</sup>.

## Protocol

The Ethics Board of Hasselt University and University Hospital Antwerp approved the studies. Participants gave their written informed consent to participate.

## 1. Instrument Setup

1. Remove the black protection shells from the digital retinal camera and the main block of the unit.
2. Open the battery compartment and place the battery in the camera. Do not disconnect the wire connecting the battery and the main unit.
3. Screw the camera onto the main unit and connect the two wires. Connect the main unit to the power grid and to the computer with the supplied USB cables.
4. Start the main unit by switching the on/off button to "on". Start the camera by switching the on/off button to "on".
5. Start the computer. This will prevent connection errors between the main unit and the computer.

## 2. Capturing Photograph

1. Start the Retinal Imaging Control Software (and fill in the required password). The software is a part of the digital retinal camera (see materials table for link).
2. Start the study by clicking the "Study" icon in the upper left part of the screen. For a new patient, fill in all the details such as patient ID, patient name, date of birth, etc. If the patient is already in the system, fill in the "patient ID" and use the "Search history list". Double-click on the name of the patient to start the study.
3. Ask the patient to take a seat before the camera, place his/her chin on the chin rest and the forehead against the forehead rest and "lock" the head to take a photograph.
4. Ask the patient to look straight into the lens of the camera. Move the camera in the horizontal (X-Y) plane to the right or left eye.
5. Use the chin rest to position the cornea of the patient inside the two circles that appear on the camera display. Fine-tune by using the wheel on the joystick.
6. Move the camera forward, backward, and sideways in the X-Y plane in order to position the pupil of the patient within the circles. Make sure the pupil forms a continuous circle. By doing so, the iris of the patient will be split up in two pieces.
7. Use the "back trigger" on the joystick to switch from the cornea to the retina. At this stage, the patient should observe a green light. Ask the patient to look at the green light.

8. Focus the camera by aligning the two lines that pop up when the wheel at the base of the joystick is turned. Turn the wheel until the two lines form a continuous line.
9. Use the green light to place the eye in the optimal position for a photograph. If required, move the light using the arrow buttons at the right side of the camera. Position the green light in a way that the optic disc is centered on the camera display.
10. Search for 2 white spots which appeared after switching to the retina (in step 2.7). To find the spots, move the unit in the X-Y plane. The spots are visible as a blurry stain. Move the unit forward or backwards until blurry stains turn into bright, white spots. The brighter and rounder the spots, the better the quality of the picture is. Position the spots until both are visible. Use the little wheel on the joystick to bring the spots to the middle of the camera display.
11. Confirm that the two lines (from step 2.8) form a continuous line. The optic disc is centered on the camera display and is flanked by two bright, white spots. Take the retinal photograph by firing the button on top of the joystick.
12. Save the photograph by pressing the "Study Complete" button on the lower right corner of the computer screen. Completing the study will automatically save the pictures in a map and close the study.

### 3. Analysis of Retinal Photograph

1. Determine the scale ratio by measuring the distance between the center of macula (fovea) and the center of the optic disc (blind spot). Anatomically this distance is determined to be 4,500  $\mu\text{m}$  or 2.5x the diameter of the optic disc, with the latter being approximately 1,800  $\mu\text{m}$ . Ensure the distance is measured in pixels. Calculate the scale ratio by dividing 4,500 by the distance (in pixels) between the macula and blind spot.
2. Open the retinal vessel analysis software "IVAN".  
NOTE: The software is created at the University of Wisconsin at Madison. Detailed information on the usage of IVAN is taken from the manual.
3. Fill in the scale ratio and proceed through the configuration.
4. Verify that three yellow rings appear on the retinal photograph. The scale ratio determines the radius of the inner circle and encloses the optic disc. Verify that the middle point of the inner ring is on the middle point of the optic disc. If this is not the case, adjust the location of the circle by using the cursor keys. The radii of the middle and outer circles are 2x and 3x larger than the radius of the inner circle, respectively. In this way, zones A and B are created at a fixed distance from the optic disc.
5. Check that the retinal image has the optic disc in the center of the photograph. This ensures a sharp focus of the image in zone B and this will facilitate the grading process (**Figure 4A**).
6. Observe that the software automatically detects the blood vessels and assigns these vessels as venules (**Figure 4B**).
7. Distinguish the vessels between arterioles and venules based on physiological differences. Arterioles will be indicated in red and venules in blue (**Figure 4C**). Use the following guidelines to identify each vessel:
  1. Determine the vessel color. Arterioles have a lighter orange-red color with a strong central light reflection. Veins have darker purple-red color with little or no central light reflex.
  2. Determine the course of the vessel. Arterioles tend to be straighter and smoother in outline; they are more regular in both path and outline. Venules are generally more tortuous, and more irregular in outline and diameter. Venules are broader in diameter at the disc margin than the corresponding arterioles.
  3. Identify the vessel by looking at the annotation of the preceding vessel. In principle, arterioles alternate with venules. Therefore, if a distinct venule is measured, the next vessel is more likely to be an arteriole.
  4. Define the crossing pattern. As a general rule, arterioles do not cross arterioles and venules do not cross venules. If a vessel of unknown identity crosses a venous branch within or distal to Zone B, then the unknown vessel is an arteriole. If it crosses an arteriolar branch within or distal to Zone B, then it is a venule.
  5. Identify smaller branches by tracing them proximally to their branching from a parent vessel, the identity of which may be evident from the first two guidelines. Use angles between vessels to differentiate crossings and branchings.  
NOTE: Crossings are frequently almost perpendicular ( $90^\circ$ ) or, if the two vessels are coursing in parallel, the angle of the crossing may be very shallow (less than  $30^\circ$ ). Branchings are usually somewhat less than perpendicular (with the angle between the two branches from  $30^\circ$  to  $45^\circ$ ).
  6. Select the full length of the vessel in the grading zone. Make sure that the standard deviation of the selected vessel does not exceed the value of 10. Smaller standard deviations indicate a good measurement.
8. Use the software tools to select vessels that were not selected by the software itself. The same rules apply for these vessels as for the vessels automatically selected by the software.
9. Determine Central Retinal Arteriolar and Venular Equivalent (CRAE and CRVE) automatically in IVAN.
10. Calculate the CRAE and CRVE from their respective branching daughter vessels using revised formulas of Parr and Hubbard<sup>28</sup>.  
NOTE: The relationship between trunks and branches, with empirically derived branching coefficients, is given in following two formulas to approximate vessel equivalents. IVAN uses the six largest arterioles and venules for calculating CRAE and CRVE. The formulas are applied in an iterative procedure to pair up the six largest arterioles (or venules) until the central arteriolar (or venular) vessel equivalent is obtained.  
Arterioles:  $\bar{W}=0.88*(w_1^2 + w_2^2)^{1/2}$  (1)  
Venules:  $\bar{W}=0.95*(w_1^2 + w_2^2)^{1/2}$  (2)  
where  $w_1$ ,  $w_2$ , and  $W$  are the widths of the narrower branch, the wider branch, and the parent trunk, respectively.  
NOTE: Assume that in a retinal photograph the six largest arterioles are 120, 110, 100, 90, 80, and 70  $\mu\text{m}$  wide. Put 120 and 70 into equation (1), as well as 110 and 80, and 100 and 90. After the first iteration there are three values: 122.2, 120.0, and 118.4. Perform the next iteration by pairing 122.2 and 118.4, yielding 149.8. Carry over the middle number (120.0) to the final iteration. Pair 149.8 and 120.0 to yield 168.7 for CRAE.

## Representative Results

### Repeatability of CRAE and CRVE Determination

A panel of 61 individuals between 22 to 56 years old and free of clinically diagnosed cardiovascular diseases was recruited for studying technical repeatability and within-rater variability of Central Retinal Arteriolar Equivalent (CRAE) and Central Retinal Venular Equivalent (CRVE) determinations. The fundus of the right eye of each individual was photographed twice within a time period of 5 min using a retinal camera (**Figures 1** and **2**). This procedure was done on 4 consecutive days, approximately at the same time of the day. The average coefficients of variation  $\pm$  standard deviation of the CRAE and CRVE of pictures taken within the 5-min period were  $1.76 \pm 1.71$  and  $1.78 \pm 1.51$ , respectively. Average  $\pm$  standard deviation of CRAE and CRVE values were  $151.31 \pm 13.53$  and  $213.20 \pm 18.44$ , respectively. No significant differences were observed for CRAE and CRVE values obtained on 4 consecutive days.

CRAE and CRVE values of the right eye were averaged to one CRAE and CRVE value per day. Subsequently, repeatability of the measurements was evaluated by means of the Intraclass Correlation Coefficient (ICC), a dimensionless statistic bounded by 0 and 1 that describes the reproducibility of repeated measures in a population. The measurements were done by a single rater. Hence, a one-way random effects model allowed to estimate the within-rater variability<sup>29</sup>. The ICC was 0.919 (95% CI: 0.883, 0.946) and 0.898 (95% CI: 0.854, 0.932) for CRAE and CRVE, respectively. These ICC values are well above the threshold of 0.6, which is considered to be clinically significant and the estimates both fall within the broad category as being "almost perfect" in reliability<sup>30</sup>.

### Panel Study to Investigate the Effect of Particulate Air Pollution

The study was conducted between January 2012 and May 2012 and included 84 individuals. Participants were 22 to 63 years old and free of clinically diagnosed cardiovascular diseases before and during the study period. One photograph of the fundus of the right eye was taken using a retinal camera on each of three separate examination days. The reader is referred to the paper of Louwies and collaborators for detailed information on how air pollution data was collected<sup>24</sup>. During the course of the study period, the ambient PM<sub>10</sub> and BC levels were high in Belgium due to westbound atmospheric transport of polluted air from Eastern Europe. This is visualized in a time lapse video (Supplementary information). Air pollution concentrations were assigned to each participant for 2, 4, and 6 hr preceding the retinal exam. Air pollution levels were calculated on the day of the clinical visit from midnight until the time of the retinal exam. Air pollution levels were also assigned for the previous day and two days before the retinal exam. These concentrations are summarized as: lag2h, lag4h, lag6h, lag 24h, and lag 2d. Pollutant-specific, exposure-response analysis using mixed models was performed. Details of these analyses can be found in the original publication<sup>24</sup>. There was an inverse association between CRAE and air pollution concentrations (measured as PM<sub>10</sub> and BC concentrations) in the hourly and daily exposure windows before the clinical examination. A decrease in CRAE of 0.93  $\mu\text{m}$  (95% CI:  $-1.42, -0.45$ ;  $p = 0.0003$ ) was observed for each 10- $\mu\text{g}/\text{m}^3$  increase in average PM<sub>10</sub> during 24 hr preceding the examination (**Figure 3**). Shorter hourly PM<sub>10</sub> exposure windows and PM<sub>10</sub> concentrations averaged over the previous 2 days also revealed a significant decrease of the CRAE values. A decrease in CRAE of 1.84  $\mu\text{m}$  (95% CI:  $-3.18, -0.51$ ;  $p = 0.008$ ) was also found for each 1- $\mu\text{g}/\text{m}^3$  increase in BC 24 hr before the examination. No additional significant associations were observed between CRAE and the other calculated BC exposure windows. A decrease in CRVE of 0.86  $\mu\text{m}$  (95% CI:  $-1.42, -0.30$ ;  $p = 0.004$ ) was observed for every 10- $\mu\text{g}/\text{m}^3$  increase in PM<sub>10</sub> in the 24 hr exposure window before the retinal picture was taken. Shorter exposure windows revealed additional significant effects (**Figure 3**). A negative association between CRVE and BC exposure during the 24 hr before the examination was observed. However, the effect did not reach the level of statistical significance ( $-1.18 \mu\text{m}$ ; 95% CI:  $-3.11, 0.75$ ;  $p = 0.23$ ).

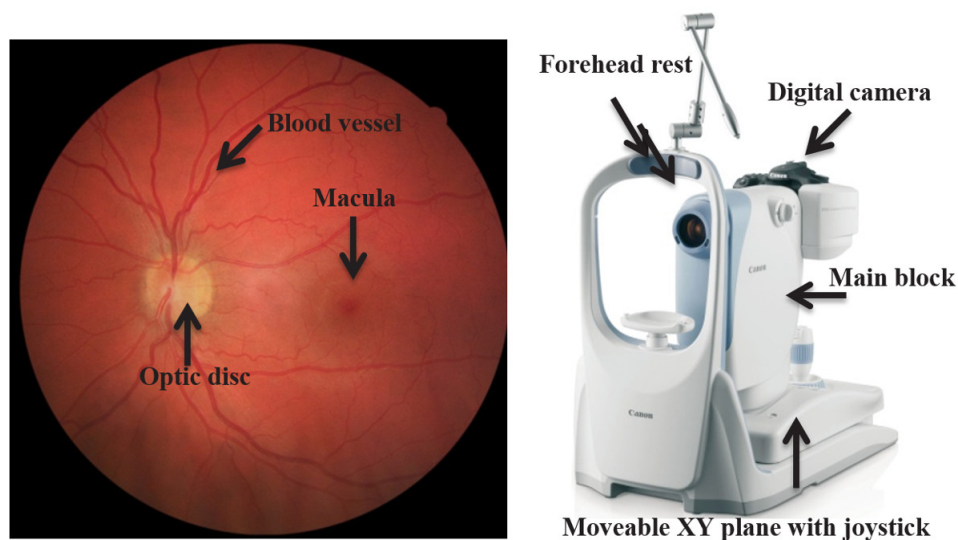


**Figure 1. Retina picture and example of a retinal camera.** Annotated retinal fundus picture of the right eye of a healthy volunteer (Left) and a picture of a non-mydiatric digital retinal camera (Right). [Please click here to view a larger version of this figure.](#)





**Figure 2. Screen shot of IVAN software.** Example of a picture that is processed with the IVAN software. The software identifies the vasculature and calculates diameters. The operator supervises the results and identifies arteries (shown in red) and venules (shown in blue). CRAE and CRVE are then calculated automatically. [Please click here to view a larger version of this figure.](#)

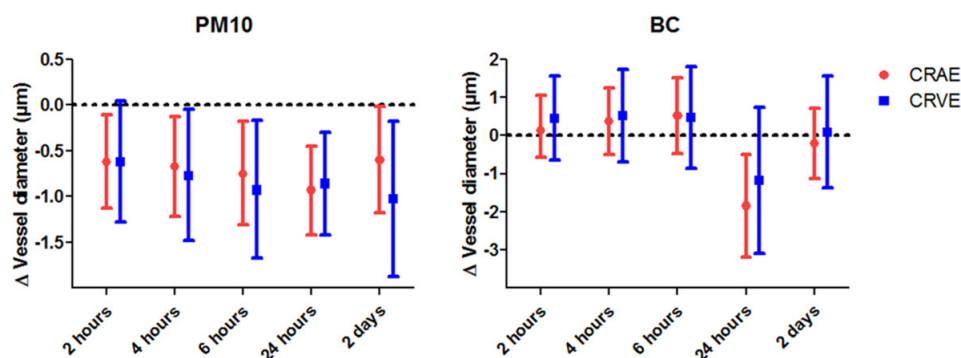


**Figure 3. Association between air pollution and retinal vessel calibers.** Estimated change in mean CRAE and CRVE (95% CI) in association with a 10-µg/m³ increase in PM<sub>10</sub> (Left) or a 1-µg/m³ increase in BC (Right) for different exposure lags. The data were obtained from a panel of 84 persons. [Please click here to view a larger version of this figure.](#)

Figure 4.A.

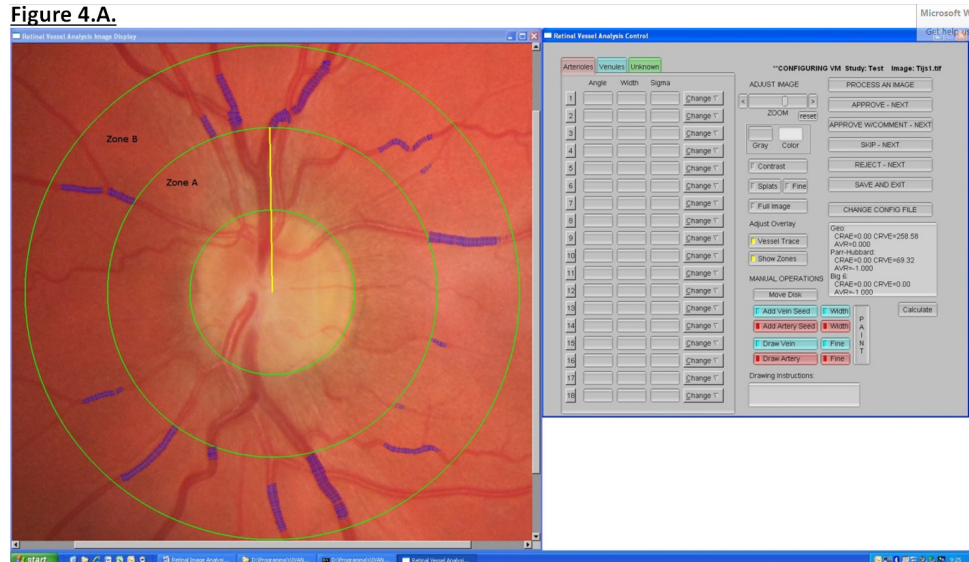


Figure 4.B.

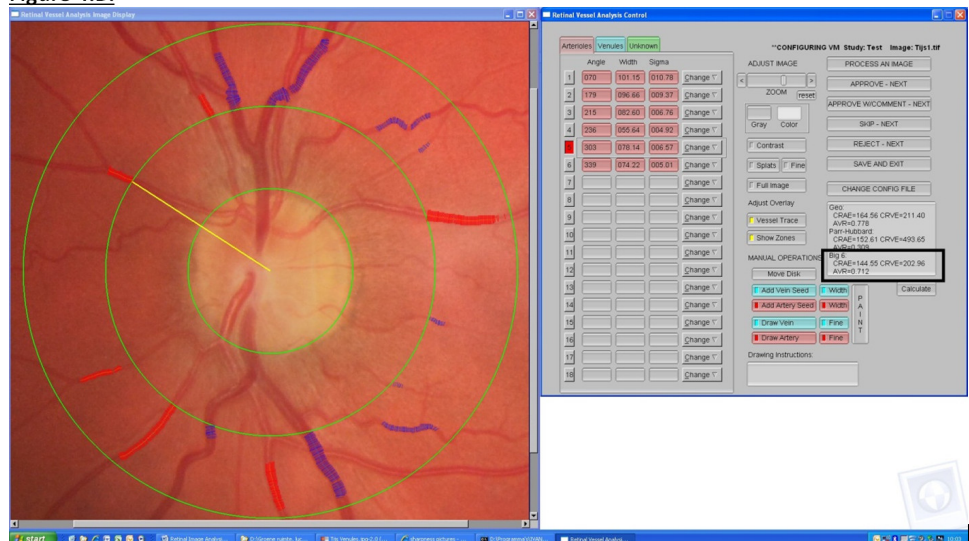


Figure 4.C.

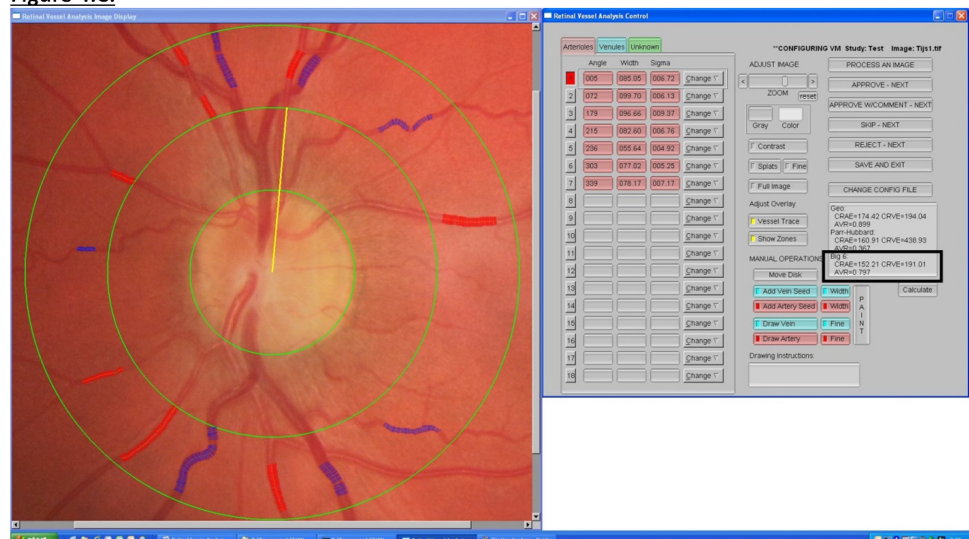


Figure 4. Please click here to view a larger version of this figure.

**Supplemental video. Time lapse video of air pollution concentrations during the panel study.**

## Discussion

Retina image analysis is proposed as a convenient tool for studying microvascular responses in epidemiological studies. When the operator is experienced, it takes less than 5 min to take a fundus picture. Furthermore, this unobtrusive procedure for visualizing the microcirculation can be used for participants from early age up to old age.

Literature is increasing with respect to the associations between morphological changes in the retinal vasculature (for example change in vessel caliber, geometric pattern, etc.) and modifiable lifestyle and environmental risk factors<sup>15,16</sup>. Experimental and epidemiological works show that short-term and long-term air pollution exposure is strongly associated with cardiovascular morbidity and mortality. However, a convenient technique such as retinal fundus photography has been used very little to study microcirculatory effects that may be induced by air pollutants.

The different steps that are required for obtaining a high-quality fundus picture are explained in this video protocol. Subsequently, the methodology is given for obtaining arteriolar and venular caliber measurements, and more specifically the Central Retinal Arteriolar Equivalent (CRAE) and the Central Retinal Venular Equivalent (CRVE)<sup>13,28</sup>. The results of the repeated measures analysis showed that the within-rater results for CRAE and CRVE are highly reproducible for pictures that were taken within a timeframe of four days. These findings are in line with the recent observations reported by McCanna and colleagues. The latter authors reported that CRAE and CRVE values are stable over a period of one month. They reported correlations for pairs of study visits of 0.9 and the correlations decreased slightly with an increasing length of time interval<sup>31</sup>.

Subsequently, it is shown in a panel study with healthy adults that the retinal microcirculation can respond rapidly to particulate matter air pollution. More specifically, a decrease in CRAE that relates to an increased short-term exposure to PM<sub>10</sub> and BC is reported<sup>24</sup>. Narrowing of retinal arterioles is a proxy for estimating the risk of cardiovascular disease and cardiovascular mortality<sup>32-35</sup>. It is envisioned that retinal microvasculature can be used to probe for cardiovascular effects of air pollution. In this respect, Adar and colleagues reported for the first time about the short-term effects of air pollution on the human retinal microvasculature in a cross-sectional analysis of the MESA cohort<sup>21</sup>. The microvascular changes reported by Louwies *et al.* (2013) complement those found by Adar *et al.* (2010). The latter authors reported a 0.4  $\mu\text{m}$ -decrease in CRAE (95% CI: -0.8, -0.04) per 9- $\mu\text{g}/\text{m}^3$  increase in average PM<sub>2.5</sub> on the previous day. Based on repeated measurements, Louwies *et al.* (2013) reported an estimate of -1.2  $\mu\text{m}$  (95% CI: -1.61, -0.61) and it is suggested that the larger effect size may be due to greater variation in PM and BC exposure concentrations in this panel study<sup>24</sup>.

Pulmonary inflammation and low-grade, systemic inflammation have been associated with exposure to air pollution<sup>36</sup>. Systemic inflammation has also been linked with endothelial dysfunction<sup>37,38</sup>. This process may affect the reactivity of retinal blood vessels<sup>39</sup>. It is assumed that inflammatory responses lead to altered endothelial activity, which may be reflected in the narrowing of the arteriolar calibers. The findings from the panel study suggest that this might occur in a timeframe of less than 24 hr because exposure to PM<sub>10</sub> was inversely associated with CRAE during all the hourly exposure windows. The observations are in line with the known impact of air pollution on health. Short-term animal studies with exposure to peak levels of air pollutants have revealed that the microvasculature can be affected<sup>40,41</sup>. In addition, human intervention studies in controlled environment have shown that endothelial function is impaired upon exposure to diesel exhaust<sup>42,43</sup>.

In conclusion, many developmental and anatomical similarities exist between retinal blood vessels and the microvasculature of the heart, lungs, and brain<sup>10</sup>. Therefore, the retinal blood vasculature is considered a surrogate tissue for the systemic microcirculation. A change in retinal blood vessels may be a valuable predictor for cardiovascular disease development. The convenient and unobtrusive analysis of retinal images is now considered useful for population-based studies with a focus on cardiovascular epidemiology. This protocol paper should encourage more research groups to use fundus photography to study microvascular effects of environmental and lifestyle factors.

## Disclosures

The authors declare they have no actual or potential competing financial interests.

## Acknowledgements

The results about the microvascular response to particulate air pollution are reproduced with permission from Environmental Health Perspectives<sup>24</sup>. The validated meteorological and air quality data were kindly provided by The Belgian Royal Meteorological Institute and the Flemish Environmental Agency. The retinal image analysis software was obtained from Dr. N. Ferrier (Madison School of Engineering and the Fundus Photograph Reading Center, Department of Ophthalmology and Visual Sciences, University of Wisconsin-Madison). Tijs Louwies and Eline Provost are supported with a VITO fellowship. Eline Provost holds an aspirant research fellowship of the Flemish Scientific Fund. Tim S. Nawrot is holder of a European Research Council starting grant.

## References

1. Clough, G., & Cracowski, J. L. Spotlight Issue: Microcirculation-From a Clinical Perspective. *Microcirculation*. **19**, 1-4, doi:10.1111/j.1549-8719.2011.00142.x (2012).
2. Tsai, A. G., Johnson, P. C., & Intaglietta, M. Oxygen gradients in the microcirculation. *Physiological Reviews*. **83**, 933-963, doi:10.1152/physrev.00034.2002 (2003).
3. Safar, M. E., & Lacolley, P. Disturbance of macro- and microcirculation: relations with pulse pressure and cardiac organ damage. *American Journal of Physiology-Heart and Circulatory Physiology*. **293**, H1-H7, doi:10.1152/ajpheart.00063.2007 (2007).



4. Abramoff, M. D., Garvin, M. K., & Sonka, M. Retinal imaging and image analysis. *IEEE reviews in biomedical engineering*. **3**, 169-208, doi:10.1109/RBME.2010.2084567 (2010).
5. Tielsch, J. M. *et al.* A population-based evaluation of glaucoma screening-the Baltimore eye survey. *American Journal of Epidemiology*. **134**, 1102-1110 (1991).
6. Ciulla, T. A., Amador, A. G., & Zinman, B. Diabetic retinopathy and diabetic macular edema - Pathophysiology, screening, and novel therapies. *Diabetes Care*. **26**, 2653-2664, doi:10.2337/diacare.26.9.2653 (2003).
7. De Silva, D. A. *et al.* Associations of retinal microvascular signs and intracranial large artery disease. *Stroke*. **42**, 812-814, doi:10.1161/STROKEAHA.110.589960 [pii] 10.1161/STROKEAHA.110.589960 (2011).
8. Liew, G. *et al.* Differing associations of white matter lesions and lacunar infarction with retinal microvascular signs. *International journal of stroke : official journal of the International Stroke Society*, doi:10.1111/j.1747-4949.2012.00865.x (2012).
9. Cheung, C. Y. *et al.* Microvascular network alterations in the retina of patients with Alzheimer's disease. *Alzheimer's & dementia : the journal of the Alzheimer's Association*. **10**, 135-142, doi:10.1016/j.jalz.2013.06.009 (2014).
10. Liew, G., Wang, J. J., Mitchell, P., & Wong, T. Y. Retinal Vascular Imaging A New Tool in Microvascular Disease Research. *Circulation-Cardiovascular Imaging*. **1**, 156-161, doi:10.1161/circimaging.108.784876 (2008).
11. McGeechan, K., Liew, G., & Wong, T. Y. Are retinal examinations useful in assessing cardiovascular risk? *Am J Hypertens*. **21**, 847; author reply 848, doi:ajh2008201 [pii] 10.1038/ajh.2008.201 (2008).
12. McClintic, B. R., McClintic, J. I., Bisognano, J. D., & Block, R. C. The relationship between retinal microvascular abnormalities and coronary heart disease: a review. *The American Journal of Medicine*. **123**, e1-e374 (2010).
13. Hubbard, L. D. *et al.* Methods for evaluation of retinal microvascular abnormalities associated with hypertension/sclerosis in the atherosclerosis risk in communities study. *Ophthalmology*. **106**, 2269-2280, doi:10.1016/s0161-6420(99)90525-0 (1999).
14. Niemeijer, M., van Ginneken, B., Russell, S. R., Suttrop-Schulten, M. S. A., & Abramoff, M. D. Automated detection and differentiation of drusen, exudates, and cotton-wool spots in digital color fundus photographs for diabetic retinopathy diagnosis. *Investigative ophthalmology & visual science*. **48**, 2260-2267, doi:10.1167/iops.06-0996 (2007).
15. Serre, K., & Sasongko, M. B. Modifiable Lifestyle and Environmental Risk Factors Affecting the Retinal Microcirculation. *Microcirculation*. **19**, 29-36, doi:10.1111/j.1549-8719.2011.00121.x (2012).
16. Sun, C., Wang, J. J., Mackey, D. A., & Wong, T. Y. Retinal Vascular Caliber: Systemic, Environmental, and Genetic Associations. *Survey of Ophthalmology*. **54**, 74-95, doi:10.1016/j.survophthal.2008.10.003 (2009).
17. Nawrot, T. S. *et al.* Stronger associations between daily mortality and fine particulate air pollution in summer than in winter: evidence from a heavily polluted region in western Europe. *Journal of Epidemiology and Community Health*. **61**, 146-149, doi:10.1136/jech.2005.044263 (2007).
18. Zanobetti, A. *et al.* The temporal pattern of respiratory and heart disease mortality in response to air pollution. *Environmental Health Perspectives*. **111**, 1188-1193, doi:10.1289/ehp.5712 (2003).
19. Brook, R. D. *et al.* Particulate Matter Air Pollution and Cardiovascular Disease An Update to the Scientific Statement From the American Heart Association. *Circulation*. **121**, 2331-2378, doi:10.1161/CIR.0b013e3181d8bec1 (2010).
20. Nawrot, T. S., Perez, L., Kunzli, N., Munters, E., & Nemery, B. Public health importance of triggers of myocardial infarction: a comparative risk assessment. *Lancet*. **377**, 732-740, doi:10.1016/s0140-6736(10)62296-9 (2011).
21. Adar, S. D. *et al.* Air Pollution and the Microvasculature: A Cross-Sectional Assessment of *In Vivo* Retinal Images in the Population-Based Multi-Ethnic Study of Atherosclerosis (MESA). *Plos Medicine*. **7**, doi:10.1371/journal.pmed.1000372 (2010).
22. Klein, R., Klein, B. E., Knudtson, M. D., Wong, T. Y., & Tsai, M. Y. Are inflammatory factors related to retinal vessel caliber? The Beaver Dam Eye Study. *Archives of ophthalmology*. **124**, 87-94, doi:10.1001/archophth.124.1.87 (2006).
23. Harris, B. *et al.* The association of systemic microvascular changes with lung function and lung density: a cross-sectional study. *PloS one* **7**, e50224, doi:10.1371/journal.pone.0050224 (2012).
24. Louwies, T., Panis, L. I., Kicinski, M., De Boever, P., & Nawrot, T. S. Retinal Microvascular Responses to Short-Term Changes in Particulate Air Pollution in Healthy Adults. *Environmental Health Perspectives*. **121**, 1011-1016, doi:10.1289/ehp.1205721 (2013).
25. Barrett, J. R. Particulate Matter and Cardiovascular Disease Researchers Turn an Eye toward Microvascular Changes. *Environmental Health Perspectives*. **121**, A282-A282, doi:10.1289/ehp.121-A282 (2013).
26. Gopinath, B. *et al.* Is quality of diet associated with the microvasculature? An analysis of diet quality and retinal vascular calibre in older adults. *The British journal of nutrition*. **110**, 739-746, doi:10.1017/s0007114512005491 (2013).
27. Kandasamy, Y., Smith, R., & Wright, I. M. Relationship between the retinal microvasculature and renal volume in low-birth-weight babies. *American journal of perinatology*. **30**, 477-481, doi:10.1055/s-0032-1326993 (2013).
28. Knudtson, M. D. *et al.* Revised formulas for summarizing retinal vessel diameters. *Current Eye Research*. **27**, 143-149, doi:10.1076/ceyr.27.3.143.16049 (2003).
29. Shrout, P. E., & Fleiss, J. L. Intraclass correlations: uses in assessing rater reliability. *Psychological bulletin*. **86**, 420-428 (1979).
30. Landis, J. R., & Koch, G. G. The measurement of observer agreement for categorical data. *Biometrics*. **33**, 159-174 (1977).
31. McCanna, C. D. *et al.* Variability of measurement of retinal vessel diameters. *Ophthalmic epidemiology*. **20**, 392-401, doi:10.3109/09286586.2013.848459 (2013).
32. Cheung, N. *et al.* Arterial compliance and retinal vascular caliber in cerebrovascular disease. *Annals of Neurology*. **62**, 618-624, doi:10.1002/ana.21236 (2007).
33. Wong, T. Y. *et al.* Retinal microvascular abnormalities and incident stroke: the atherosclerosis risk in communities study. *Lancet*. **358**, 1134-1140, doi:10.1016/s0140-6736(01)06253-5 (2001).
34. Wong, T. Y. *et al.* Retinal arteriolar narrowing and risk of coronary heart disease in men and women - The atherosclerosis risk in communities study. *Jama-Journal of the American Medical Association*. **287**, 1153-1159, doi:10.1001/jama.287.9.1153 (2002).
35. Wong, T. Y. *et al.* The prevalence and risk factors of retinal microvascular abnormalities in older persons - The cardiovascular health study. *Ophthalmology*. **110**, 658-666, doi:10.1016/s0161-6420(02)01931-0 (2003).
36. Hoffmann, B. *et al.* Chronic Residential Exposure to Particulate Matter Air Pollution and Systemic Inflammatory Markers. *Environmental Health Perspectives*. **117**, 1302-1308, doi:10.1289/ehp.0800362 (2009).
37. Hingorani, A. D. *et al.* Acute systemic inflammation impairs endothelium-dependent dilatation in humans. *Circulation*. **102**, 994-999 (2000).
38. Huang, A. L., & Vita, J. A. Effects of systemic inflammation on endothelium-dependent vasodilation. *Trends in Cardiovascular Medicine*. **16**, 15-20, doi:10.1016/j.tcm.2005.10.002 (2006).



39. Nguyen, T. T. *et al.* Flicker light-induced retinal vasodilation in diabetes and diabetic retinopathy. *Diabetes Care*. **32**, 2075-2080, doi:10.2337/dc09-0075 (2009).
40. Nurkiewicz, T. R., Porter, D. W., Barger, M., Castranova, V., & Boegehold, M. A. Particulate matter exposure impairs systemic microvascular endothelium-dependent dilation. *Environmental Health Perspectives*. **112**, 1299-1306, doi:10.1289/ehp.7001 (2004).
41. Nurkiewicz, T. R. *et al.* Systemic microvascular dysfunction and inflammation after pulmonary particulate matter exposure. *Environmental Health Perspectives*. **114**, 412-419, doi:10.1289/ehp.8413 (2006).
42. Barath, S. *et al.* Impaired vascular function after exposure to diesel exhaust generated at urban transient running conditions. *Particle and Fibre Toxicology*. **7**, doi:10.1186/1743-8977-7-19 (2010).
43. Tornqvist, H. *et al.* Persistent endothelial dysfunction in humans after diesel exhaust inhalation. *American Journal of Respiratory and Critical Care Medicine*. **176**, 395-400, doi:10.1164/rccm.200606-872OC (2007).